

Nickel(II)- α -diimine complexes containing naphthyl substituents for ethylene polymerization under low ethylene pressure

Jianchao Yuan · Zong Jia · Jing Li ·
Fengying Song · Fuzhou Wang · Bingnian Yuan

Received: 22 November 2012 / Accepted: 15 January 2013 / Published online: 26 January 2013
© Springer Science+Business Media Dordrecht 2013

Abstract Two new α -diimine containing Ni(II) complexes, {bis[*N,N'*-(2,6-dimethyl-4-naphthylphenyl)imino]-1,2-dimethylethane}dibromonickel **3a** and {bis[*N,N'*-(2-methyl-4-naphthylphenyl)imino]-1,2-dimethylethane}dibromonickel **3b** were synthesized and characterized. The crystal structures of representative ligand **2a** and its complex **3a** were determined by X-ray crystallography. Complex **3a** bearing 2,6-dimethyl and 4-naphthyl groups, activated by diethylaluminum chloride (DEAC), shows high catalytic activity for the polymerization of ethylene [4.43×10^6 g PE/(mol Ni h bar)]. Interestingly, complexes **3a** and **3b** bearing the naphthyl substituent in the *para*-aryl position produced dendritic polyethylenes (branching degree, **3a**: 112, 118, and 147; **3b**: 113, 127, and 151 branches/1,000 C at 20, 40, and 60 °C, respectively). The dendritic polyethylene particle size obtained by **3a** and **3b**/DEAC can be controlled in the 1–20 nm range under low ethylene pressure (diameter, **3a**: 18.31, 14.44, and 11.09; **3b**: 12.29, 8.98 and 6.27 nm at 20, 40, and 60 °C, respectively) and could be expected to produce a nano-targeted drug carrier after modification with water-soluble oligo(ethylene glycol).

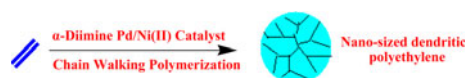
Introduction

“Chain walking polymerization CWP” catalyzed by Ni(II)/Pd(II)- α -diimine complexes has attracted increasing attention due to its ability to produce hyperbranched or dendritic polymer under low ethylene pressure [1–24] (Scheme 1). Nanosized dendrimers are artificial macromolecules with tree-like structures and are synthesized from branched monomer units in a stepwise manner [25]. Due to their surface functional groups and highly branched architectures, nanosized dendrimers have an enormous capacity for solubilization of hydrophobic drugs and can be modified or conjugated with various interesting guest molecules [25, 26]. Based on the “enhanced permeability and retention (EPR) effect” [27–30], the nanosized dendrimers have shown great promise in the development of anticancer drug delivery systems [31]. However, it is very difficult to prepare dendrimers through stepwise synthesis. Chain-walking ethylene polymerization with Ni(II)/Pd(II)- α -diimine catalysts represents a new concept for the synthesis of hyperbranched or dendritic polyethylenes. CWP followed by atom transfer radical polymerization (ATRP) can efficiently synthesize water-soluble core-shell [core: polyethylene, PE; shell: oligo(ethylene glycol), OEG] dendritic nanoparticles with tunable sizes and reactive surface functionalities [32], which could play a very important role in tumor-targeted anticancer drugs. A key part of this approach is the synthesis of highly active late transition metal catalysts, which could produce dendritic polyethylene and control the polyethylene particle diameter in the nanometer range.

In this work, we first report the synthesis and characterization of two new α -diimine Ni(II) complexes of the type [NiBr₂(Ar-DAB)] (Ar-DAB = *N,N'*-diaryl-1,4-diaza-1,3-butadiene) bearing very bulky naphthyl groups (naphthyl

Electronic supplementary material The online version of this article (doi:10.1007/s11243-013-9699-3) contains supplementary material, which is available to authorized users.

J. Yuan (✉) · Z. Jia · J. Li · F. Song · F. Wang · B. Yuan
Key Laboratory of Eco-Environment-Related Polymer Materials,
Ministry of Education, Key Laboratory of Polymer Materials
of Gansu Province, College of Chemistry and Chemical
Engineering, Northwest Normal University,
Lanzhou 730070, China
e-mail: jianchaoyuan@nwnu.edu.cn



Scheme 1 Synthesis of nanosized polyethylene

group may behave either as an electron donor or as an electron attractor) in the *para*-aryl position and different groups (one or two electron-donating methyl groups) in the *ortho*-aryl position of the arylimino group, in order to study the influence of different steric effects and electron densities at the metal center on the catalyst activity and, in particular, on the microstructure and size of polyethylene.

Experimental

General procedures and materials

All manipulations involving air and/or moisture-sensitive compounds were carried out with standard Schlenk techniques under nitrogen. Methylene chloride and *o*-dichlorobenzene were pre-dried with 4 Å molecular sieves and distilled from CaH₂ under dry nitrogen. Toluene, diethyl ether, and 1,2-dimethoxyethane (DME) were distilled from sodium/benzophenone under N₂ atmosphere. Anhydrous NiBr₂ (99 %), 1-naphthyl boric acid (97 %), Pd(OAc)₂, and diethylaluminum chloride (DEAC, 0.9 M solution in toluene) were obtained from Acros. 2,3-Butanedione (98 %), 2,6-dimethylbenzenamine (98 %), 4-bromo-2-methylbenzenamine (98 %), and 4-bromo-2,6-dimethylbenzenamine (98 %) were purchased from Alfa Aesar and used without further purification. [NiBr₂(DME)] was synthesized according to the literature [33].

NMR spectra were recorded at 400 MHz on a Varian Mercury Plus-400 instrument, using TMS as internal standard. FTIR spectra were recorded on a Digilab Merlin FTS 3000 FTIR spectrophotometer on KBr pellets. The molecular weights and molecular weight distributions (M_w/M_n) of the polymers were determined by gel permeation chromatography/size-exclusion chromatography (GPC/SEC) via a Waters Alliance GPCV2000 chromatograph, using 1,2,4-trichlorobenzene as eluent, at a flow rate of 1.0 ml/min and operated at 140 °C. Effective hydrodynamic diameters of the dendritic polyethylenes (1 mg/ml in *o*-dichlorobenzene) were measured using a Zeta-pals dynamic light-scattering detector (Brookhaven Instruments, Holtsville, NY, USA) with a 15 mV incident beam at 676 nm at 20 °C. Correlation functions were collected at a scattering angle of 90°. Particle sizes were calculated using the multiple angle sizing option of the instrument's particle sizing software.

Synthesis of 2,6-dimethyl-4-naphthylbenzenamine **1a**

Pd(OAc)₂ (0.01 g, 0.04 mmol), 4-bromo-2,6-dimethylbenzenamine (0.40 g, 2.00 mmol), K₂CO₃ (0.55 g, 4.00 mmol),

and 1-naphthyl boric acid (0.38 g, 2.20 mmol) were placed in a 100-ml flask and allowed to stir at 25 °C for 24 h, in the presence of 10 ml PEG-400. The mixture was extracted three times with 15 ml diethyl ether. The combined organic phase was dried over MgSO₄, filtered, and the solvent was removed. The residue was purified by chromatography on silica gel with petroleum ether/ethyl ester (v/v = 50:1) to give 2,6-dimethyl-4-naphthylbenzenamine (0.35 g, 71 % yield). ¹H NMR (400 MHz, CDCl₃): δ 2.30 (s, 6H, -CH₃), 4.13 (s, 2H, -NH₂), 7.12 (s, 2H, benzenamine), 7.36–7.51 (m, 3H, naphthyl), 7.81 (d, 2H, naphthyl), 7.90 (d, 1H, naphthyl), 8.01 (d, 1H, naphthyl). ¹³C NMR (400 MHz, CDCl₃): δ 17.71 (carbon 1), 121.48 (carbon 2), 125.37 (carbon 3), 125.61 (carbon 4), 126.35 (carbon 5), 126.77 (carbon 6), 128.12 (carbon 7), 129.89 (carbon 8), 130.36 (carbon 9), 131.88 (carbon 10), 133.81 (carbon 11), 140.58 (carbon 12), 141.92 (carbon 13) (The numbered compounds are shown in Chart S1 in the Supporting Information).

Synthesis of 2-methyl-4-naphthylbenzenamine **1b**

Pd(OAc)₂ (0.01 g, 0.04 mmol), 4-bromo-2-methylbenzenamine (0.56 g, 3.00 mmol), K₂CO₃ (0.55 g, 4.00 mmol), and 1-naphthyl boric acid (0.57 g, 3.30 mmol) were placed in a 100-ml flask and allowed to stir at 25 °C for 24 h, in the presence of 10 ml PEG-400. The mixture was extracted three times with 15 ml diethyl ether. The combined organic phase was dried over MgSO₄, filtered, and the solvent was removed. The residue was purified by chromatography on silica gel with petroleum ether/ethyl ester (v/v = 30:1) to give 2-methyl-4-naphthylbenzenamine (0.42 g, 60 % yield). ¹H NMR (400 MHz, CDCl₃): δ 2.12 (s, 3H, -CH₃), 3.61 (s, 2H, -NH₂), 6.55 (d, 1H, benzenamine), 6.81 (s, 1H, benzenamine), 6.83 (d, 1H, benzenamine), 7.30–7.51 (m, 3H, naphthyl), 7.82 (d, 2H, naphthyl), 7.93 (d, 1H, naphthyl), 8.00 (d, 1H, naphthyl). ¹³C NMR (400 MHz, CDCl₃): δ 17.18 (carbon 1), 110.08 (carbon 2), 114.77 (carbon 3), 116.31 (carbon 4), 122.17 (carbon 5), 124.42 (carbon 6), 125.51 (carbon 7), 126.27 (carbon 8), 126.73 (carbon 9), 126.90 (carbon 10), 128.16 (carbon 11), 128.64 (carbon 12), 129.52 (carbon 13), 132.12 (carbon 14), 132.79 (carbon 15) (The numbered compounds are shown in Chart S1 in the Supporting Information).

Synthesis of bis[*N,N'*-(2,6-dimethyl-4-naphthylphenyl)imino]-1,2-dimethylethane **2a**

Formic acid (0.5 ml) was added to a stirred solution of 2,3-butanedione (0.09 g, 1.00 mmol) and 2,6-dimethyl-4-naphthylbenzenamine (0.49 g, 2.00 mmol) in methanol (50 ml). The mixture was refluxed for 48 h, cooled, and the precipitate was separated by filtration. The solid was recrystallized from EtOH/CHCl₂ (v/v = 10:1), washed, and

dried under vacuum. Yield: 0.30 g (55 %). ^1H NMR (400 MHz, CDCl_3): δ 2.15 (s, 12H, $-\text{CH}_3$ of benzenamine), 2.22 (s, 6H, $-\text{N}=\text{C}(\text{CH}_3)-\text{C}(\text{CH}_3)=\text{N}-$), 7.25 (s, 4H, benzenamine ring), 7.45–7.55 (m, 6H, naphthyl), 7.86 (d, 4H, naphthyl), 7.92 (d, 2H, naphthyl), 8.03 (d, 2H, naphthyl). ^{13}C NMR (400 MHz, CDCl_3): δ 16.13 (carbon 1), 17.95 (carbon 2), 124.59 (carbon 3), 125.64 (carbon 4), 126.25 (carbon 5), 126.80 (carbon 6), 128.21 (carbon 7), 129.66 (carbon 8), 131.86 (carbon 9), 132.54 (carbon 10), 133.82 (carbon 11), 135.74 (carbon 12), 140.34 (carbon 13), 147.48 (carbon 14), 168.31 (carbon 15) (The numbered compounds are shown in Chart S1 in the Supporting Information). Anal. Calcd. for $\text{C}_{40}\text{H}_{36}\text{N}_2$: C, 88.20; H, 6.66; N, 5.14. Found: C, 88.43; H, 6.47; N, 5.01. Single crystals of ligand **2a** suitable for X-ray analysis were obtained at -30°C by dissolving the ligand in CH_2Cl_2 , followed by slow layering of the resulting solution with *n*-hexane.

Synthesis of bis[*N,N'*-(2-methyl-4-naphthylphenyl)imino]-1,2-dimethylethane **2b**

Formic acid (0.5 ml) was added to a stirred solution of 2,3-butanedione (0.12 g, 1.40 mmol) and 2-methyl-4-naphthylbenzenamine (0.65 g, 2.80 mmol) in methanol (50 ml). The mixture was refluxed for 48 h, cooled, and the precipitate was separated by filtration. The solid was recrystallized from $\text{EtOH}/\text{CHCl}_3$ (v/v = 10:1), washed, and dried under vacuum. Yield: 0.41 g (57 %). ^1H NMR (400 MHz, CDCl_3): δ 2.24 (s, 6H, CH_3 of benzenamine), 2.30 (s, 6H, $-\text{N}=\text{C}(\text{CH}_3)-\text{C}(\text{CH}_3)=\text{N}-$), 6.82 (d, 2H, benzenamine), 7.26 (s, 2H, benzenamine), 2.28 (d, 2H, benzenamine), 7.35–7.56 (m, 6H, naphthyl), 7.87 (d, 4H, naphthyl), 7.93 (d, 2H, naphthyl), 8.02 (d, 2H, naphthyl). ^{13}C NMR (400 MHz, CDCl_3): δ 15.82 (carbon 1), 17.94 (carbon 2), 117.16 (carbon 3), 125.39 (carbon 4), 125.69 (carbon 5), 126.14 (carbon 6), 126.86 (carbon 7), 127.37 (carbon 8), 128.17 (carbon 9), 128.66 (carbon 10), 131.79 (carbon 11), 132.10 (carbon 12), 133.82 (carbon 13), 136.40 (carbon 14), 140.14 (carbon 15), 148.56 (carbon 16), 167.87 (carbon 17) (The numbered compounds are shown in Chart S1 in the Supporting Information). Anal. Calcd. for $\text{C}_{38}\text{H}_{32}\text{N}_2$: C, 88.34; H, 6.24; N, 5.42. Found: C, 88.15; H, 6.42; N, 5.21.

Synthesis of bis[*N,N'*-(2,6-dimethylphenyl)imino]-1,2-dimethylethane **2c**

Formic acid (0.5 ml) was added to a stirred solution of 2,3-butanedione (0.35 g, 4.00 mmol) and 2,6-dimethylbenzenamine (0.97 g, 8.00 mmol) in methanol (30 ml). The mixture was stirred at 45°C for 24 h, cooled, and the precipitate was filtered off. The solid was recrystallized from $\text{EtOH}/\text{CH}_2\text{Cl}_2$ (v/v = 10:1), washed with cold

ethanol, and dried under vacuum. Yield: 1.16 g (88 %). ^1H NMR (400 MHz, CDCl_3): δ 2.00 (s, 12H, $-\text{CH}_3$ of benzenamine), 2.35 (s, 6H, $-\text{N}=\text{C}(\text{CH}_3)-\text{C}(\text{CH}_3)=\text{N}-$), 6.96 (d, 4H, benzenamine ring near methyl), 7.08 (t, benzenamine). ^{13}C NMR (100 MHz, CDCl_3): δ 15.80 (carbon 1), 17.78 (carbon 2), 123.22 (carbon 3), 124.63 (carbon 4), 127.90 (carbon 5), 148.30 (carbon 6), 168.03 (carbon 7) (The numbered compounds are shown in Chart S1 in the Supporting Information). Anal. Calcd. for $\text{C}_{20}\text{H}_{24}\text{N}_2$: C, 82.15; H, 8.27; N, 9.58. Found: C, 82.27; H, 8.14; N, 9.43.

Synthesis of {bis[*N,N'*-(2,6-dimethyl-4-naphthylphenyl)imino]-1,2-dimethylethane}dibromonickel **3a**

$\text{NiBr}_2(\text{DME})$ (0.31 g, 1.00 mmol), ligand **2a** (0.54 g, 1.00 mmol), and dichloromethane (40 ml) were mixed in a Schlenk flask and stirred at room temperature for 24 h. The resulting suspension was filtered. The solvent was removed under vacuum, and the residue was washed with diethyl ether (3×15 ml) and then dried under vacuum at room temperature to give complex **3a** 0.66 g (86 % yield). Anal. Calcd. for $\text{C}_{40}\text{H}_{36}\text{Br}_2\text{N}_2\text{Ni}$: C, 62.95; H, 4.75; N, 3.67. Found: C, 62.81; H, 4.62; N, 3.54. FT-IR (KBr) $1,631\text{ cm}^{-1}$ (C=N). Single crystals of complex **3a** suitable for X-ray analysis were obtained at -30°C by dissolving the nickel complex in CH_2Cl_2 , following by slow layering of the resulting solution with *n*-hexane.

Synthesis of {bis[*N,N'*-(2-methyl-4-naphthylphenyl)imino]-1,2-dimethylethane}dibromonickel **3b**

$\text{NiBr}_2(\text{DME})$ (0.31 g, 1.00 mmol), ligand **2b** (0.52 g, 1.00 mmol), and dichloromethane (40 ml) were mixed in a Schlenk flask and stirred at room temperature for 24 h. The resulting suspension was filtered. The solvent was removed under vacuum, and the residue was washed with diethyl ether (3×15 ml) and then dried under vacuum at room temperature to give complex **3b** (0.63 g, 85 % yield). Anal. Calcd. for $\text{C}_{38}\text{H}_{32}\text{Br}_2\text{N}_2\text{Ni}$: C, 62.08; H, 4.39; N, 3.81. Found: C, 61.87; H, 4.28; N, 3.95. FT-IR (KBr) $1,624\text{ cm}^{-1}$ (C=N).

Synthesis of {bis[*N,N'*-(2,6-dimethylphenyl)imino]-1,2-dimethylethane}dibromonickel **3c**

$\text{NiBr}_2(\text{DME})$ (0.31 g, 1.00 mmol), ligand **2c** (0.29 g, 1.00 mmol), and dichloromethane (40 ml) were mixed in a Schlenk flask and stirred at room temperature for 24 h. The resulting suspension was filtered. The solvent was removed under vacuum, and the residue was washed with diethyl ether (3×15 ml) and then dried under vacuum at room temperature to give catalyst **3c** 0.43 g (84 % yield). Anal.

Calcd. for $C_{20}H_{24}Br_2 N_2Ni$: C, 47.02; H, 4.73; N, 5.48. Found: C, 47.16; H, 4.59; N, 5.61. FT-IR (KBr) $1,632\text{ cm}^{-1}$ (C=N).

X-ray structure determinations

Single crystals of ligand **2a** and its complex **3a** suitable for X-ray analysis were obtained at $-30\text{ }^\circ\text{C}$ by dissolving the ligand and nickel complex in CH_2Cl_2 , followed by slow layering of the resulting solution with *n*-hexane. Data collections were performed at 296(2) K on a Bruker SMART APEX diffractometer with a CCD area detector, using graphite monochromated $MoK\alpha$ radiation ($\lambda = 0.71073\text{ \AA}$). The determination of crystal class and unit cell parameters was carried out by the SMART program package. The raw frame data were processed using SAINT and SADABS to yield the reflection data file. The structures were solved by using the SHELXTL program. Refinement was performed on F^2 anisotropically for all non-hydrogen atoms by the full-matrix least-squares method. The hydrogen atoms were placed at the calculated positions and were included in the structure calculation without further refinement of the

parameters. Crystal data, data collection, and refinement parameters are listed in Table 1.

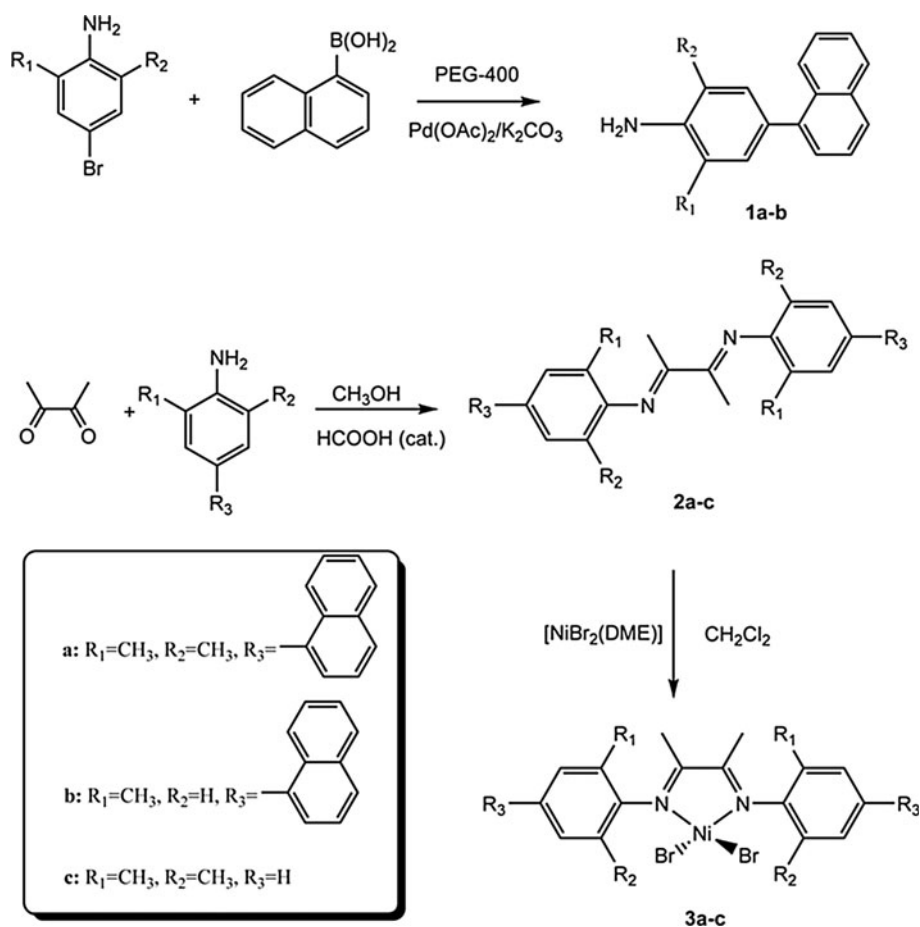
Procedure for the polymerization of ethylene

The polymerization of ethylene was carried out in a flame dried 250-ml crown-capped pressure bottle sealed with a neoprene septum. After drying the polymerization bottle under N_2 atmosphere, 50 ml of dry toluene was added to the polymerization bottle. The resulting solvent was then saturated with a prescribed ethylene pressure. The co-catalyst (DEAC) was then added in Al/Ni molar ratios in the range of 200–1,000 to the polymerization bottle via a syringe. At this time, the solutions were thermostated to the desired temperature and allowed to equilibrate for 15 min. Subsequently, an *o*-dichlorobenzene solution of Ni catalyst was added to the polymerization reactor. The polymerization, conducted under a dynamic pressure of ethylene (0.2 bar), was terminated by quenching the mixtures with 100 ml of a 2 % HCl–MeOH solution. The precipitated polymer was filtered off, washed with methanol, and dried under vacuum at $60\text{ }^\circ\text{C}$ to a constant weight.

Table 1 Crystal data and structure refinements of ligand **2a** and complex **3a**

| | | |
|--|--|---|
| Empirical formula | $C_{40}H_{36}N_2$ | $C_{40}H_{36}Br_2N_2Ni$ |
| Formula mass | 544.71 | 763.24 |
| Temperature (K) | 296 | 293 K |
| Wavelength (\AA) | 0.71073 | 0.71073 |
| Crystal size (mm^3) | $0.23 \times 0.21 \times 0.16$ | $0.20 \times 0.16 \times 0.14\text{ mm}$ |
| Crystal system | Monoclinic | Orthorhombic, P_{nma} |
| Space group | $P2_1/c$ | $P2_1/m$ |
| <i>a</i> (\AA) | 11.214(7) | 13.971(11) |
| <i>b</i> (\AA) | 9.274(6) | 28.24(2) |
| <i>c</i> (\AA) | 15.628(9) | 8.635(7) |
| <i>V</i> (\AA^3) | 1,584.9(16) | 3,407(5) |
| <i>Z</i> | 2 | 4 |
| Density (calcd.) (mg/cm^3) | 1.141 | 1.488 |
| Absorption coefficient (mm^{-1}) | 0.07 | 2.95 |
| <i>F</i> (000) | 580 | 1,552 |
| Theta range for data collection ($^\circ$) | $\theta = 2.6\text{--}25.5^\circ$ | $2.5\text{--}20.6$ |
| Limiting indices | $-8 \leq h \leq 13, -11 \leq k \leq 9, -18 \leq l \leq 18$ | $-16 \leq h \leq 15, -33 \leq k \leq 31, -8 \leq l \leq 10$ |
| Reflections collected | 1,501 | 14,330 |
| Independent reflections | 2,900 | 3,058 |
| R_{int} | 0.044 | 0.129 |
| Completeness to $\theta = 25.50^\circ$ | 98.10 % | 99.00 % |
| Final <i>R</i> indices [$I > 2\theta(I)$] | $R_1 = 0.0631, wR_2 = 0.1501$ | $R_1 = 0.0799, wR_2 = 0.1734$ |
| <i>R</i> indices (all data) | $R_1 = 0.1318, wR_2 = 0.1885$ | $R_1 = 0.1911, wR_2 = 0.2283$ |
| Refinement method | Full-matrix least-squares on F^2 | Full-matrix least-squares on F^2 |
| Goodness of fit on F^2 | 1.02 | 1.06 |
| Maximum and minimum transmission | 0.985 and 0.990 | 0.683 and 0.590 |
| Largest difference peak and hole ($e\text{ \AA}^{-3}$) | 0.27 and -0.19 | 1.16 and -0.40 |

Scheme 2 Syntheses of α -diimine ligands **2a–c** and their corresponding α -diimine nickel(II) dibromide complexes **3a–c**



Results and discussion

Synthesis and characterization of ligands **2a–c** and complexes **3a–c**

The Suzuki coupling reaction of 4-bromo-2,6-dimethylbenzenamine (4-bromo-2-dimethylbenzenamine) and 1-naphthyl boric acid catalyzed by $Pd(OAc)_2$ in PEG-400 led to the desired amine 2,6-dimethyl-4-naphthylbenzenamine **1a** (2-methyl-4-naphthylbenzenamine **1b**) in 71 % (60 %) yield (Scheme 2). The α -diimine ligands (**2a–c**) were finally obtained by acid-catalyzed condensation of the amines and 2,3-butanedione, and recrystallized from EtOH/ CH_2Cl_2 to afford microcrystalline solids. The ligands (**2a–c**) were characterized by 1H - and ^{13}C -NMR and were found to be elementally pure. Elemental analysis of ligand **2a** fits the molecular structure obtained by the X-ray structural studies (see below).

The reaction of equimolar amounts of $NiBr_2(DME)$ and the α -diimine ligands (**2a–c**) in CH_2Cl_2 led to the displacement of 1,2-DME and afforded the catalyst precursors (**3a–c**) as a moderately air-stable microcrystalline solids in high yields. Elemental analysis of complex **3a** fits the molecular structure obtained by the X-ray structural studies.

Suitable crystals of ligand **2a** and complex **3a** for X-ray diffraction were obtained at $-30\text{ }^\circ\text{C}$ by double layering a CH_2Cl_2 solution of the ligand and complex with *n*-hexane.

The molecular structure of ligand **2a** was determined and the corresponding diagram is shown in Fig. 1, while selected bond distances and angles are summarized in Table 2. The X-ray structure of **2a** exhibits *trans*-conformation about the central C–C bond of the ligand backbone. Bond lengths and angles are within the expected range for α -diimines; for example, the bond distances for the C(19)=N(1) double bond and the central C(19)–C(19a) single bond are 1.272(3) Å and 1.485(5) Å, which are very close to the values for other structurally characterized free α -diimines [34]. Both C(19) and C(1) possess essentially rather planar geometry (sp^2 character), as shown by the C(19)–N(1)–C(1) angles [121.6(2)], which are very close to 120° .

The molecular structure of complex **3a** was also determined and the corresponding diagram is shown in Fig. 2, while selected bond distances and angles are summarized in Table 2. The structure of complex **3a** has pseudo-tetrahedral geometry about the nickel center, showing C_{2v} molecular symmetry. In the solid state, the most interesting feature of ligand **2a** is the conformation of the substituents attached to N(1) and N(1a). These groups are rotated about

Fig. 1 Molecular structure of ligand **2a**. Hydrogen atoms have been omitted for clarity

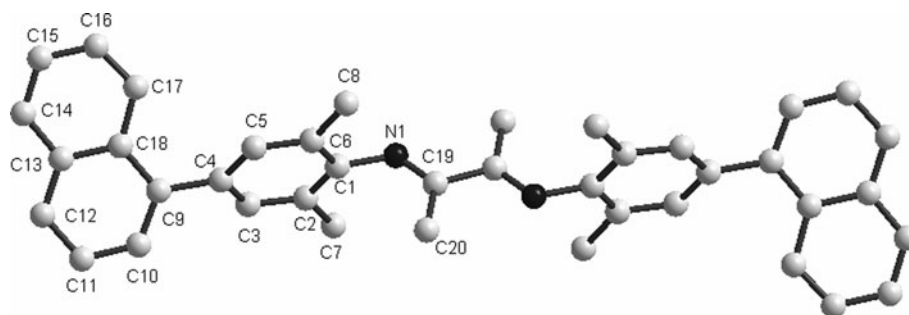


Table 2 Selected bond lengths (Å) and angles (°) for ligand **2a** and complex **3a**

| Bond lengths | (Å) | |
|--------------|------------|-----------|
| | 3a | 2a |
| Ni1–N1a | 2.001(7) | |
| Ni1–N1 | 2.001(7) | |
| Ni1–Br1 | 2.328(3) | |
| Ni1–Br2 | 2.340(3) | |
| C11–C12 | 1.382(13) | 1.380(4) |
| C11–C16 | 1.418(14) | 1.389(4) |
| C13–C14 | 1.395(12) | 1.388(4) |
| C13–C17 | 1.496(13) | 1.511(4) |
| C14–C15 | 1.395(12) | 1.391(4) |
| C14–N1 | 1.470(10) | 1.422(3) |
| C15–C18 | 1.471(13) | 1.501(4) |
| C19–N1 | 1.280(10) | 1.272(3) |
| C19–C19a | 1.537(15) | 1.485(5) |
| Bond angles | (°) | |
| N1a–Ni1–N1 | 80.2(4) | |
| N1a–Ni1–Br1 | 116.1(2) | |
| N1–Ni1–Br1 | 116.1(2) | |
| N1a–Ni1–Br2 | 110.7(2) | |
| N1–Ni1–Br2 | 110.7(2) | |
| Br1–Ni1–Br2 | 117.39(11) | |
| C13–C12–C11 | 122.6(10) | 122.1(3) |
| C12–C13–C14 | 117.5(9) | 118.9(3) |
| C12–C13–C17 | 119.6(10) | 120.6(3) |
| C14–C13–C17 | 122.8(8) | 120.5(3) |
| N1–C19–C20 | 127.2(7) | 125.3(3) |
| C20–C19–C19a | 118.5(5) | 118.4(3) |
| C19–N1–C14 | 119.7(7) | 121.6(2) |

180° from the position they must occupy to chelate a metal center. The rotation has been confirmed by the crystal structure of its complex **3a**. The X-ray structures of ligand **2a** and complex **3a** exhibit *trans*- and *cis*-conformation about the central C–C bond of the backbone, respectively. The imino C=N bond length of complex **3a** (1.280 Å) is slightly larger than that of its ligand **2a** (1.272 Å).

The C19–N1–C14 bond angle of complex **3a** (119.7°) is slightly smaller than that of its ligand **2a** (121.6°) due to the N–Ni coordination. Both aryl rings bonded to the iminic nitrogens of the α -diimine lie nearly perpendicular to the plane formed by the nickel and coordinated nitrogen atoms. The methyl groups in the 2,6-positions of the benzenamine fragments in **3a** point toward each other above and below the plane, thus shielding the apical positions of the Ni(II) center. Its structure is similar to those reported in the literature for other similar [NiBr₂(α -diimine)] compounds characterized by X-ray diffraction, {bis[*N,N'*-4-bromo-2,6-dimethylphenyl]imino]acenaphthene}dibromonickel [35] and {bis[*N,N'*-(2,4,6-trimethylphenyl)imino]acenaphthene}dibromonickel [36]. In fact, the Ni–N bond distances in complex **3a** (2.001 Å) are similar to those determined for these compounds (2.026 and 2.021 Å, respectively), as well as the Ni–Br bond distances (2.328 Å for complex **3a** vs. 2.3229 and 2.323 Å, respectively) and the N–Ni–Br angles (116.1° for complex **3a** vs. 113.32 and 114.4°, respectively).

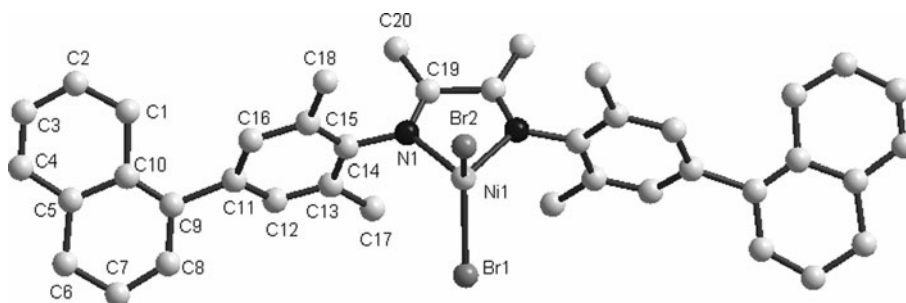
Polymerization of ethylene with nickel complexes **3a–c**

The three α -diimine nickel (II) complexes **3a–c**, activated by DEAC, were tested as catalyst precursors for the polymerization of ethylene, under the same reaction conditions. The results of the polymerization experiments are shown in Table 3. Noteworthy is the fact that blank experiments carried out with DEAC alone, under similar conditions, showed its inability to polymerize ethylene on its own.

An increase of the [Al]/[Ni] ratio in the range 200–1,000 increases slightly the activity of complexes **3a** and **3b**, at 10 °C, which seem to go through a maximum around [Al]/[Ni] = 600 (**3a**: runs 1–5; **3b**: runs 10–14). For a ratio [Al]/[Ni] = 600, the highest activities of complexes **3a** (runs 3, 6–9) and **3b** (runs 12, 15–18) appeared around 10 °C [the highest activities of complex **3c** (runs 19–22) appeared around 0 °C].

The performances of the nickel precatalysts are significantly affected by the position of the naphthyl and methyl substituents on the aryl rings of the α -diimine Ni(II) complexes **3a–c** (Table 3). Complex **3a**, bearing a naphthyl

Fig. 2 Molecular structure of complex **3a**. Hydrogen atoms have been omitted for clarity



substituent in the *para*-aryl position of the ligand (two methyl groups in the *ortho*-aryl positions), displays the highest catalytic activity, of 4.43×10^6 g PE/(mol Ni h bar), and produces one of the highest molecular weights ($M_n = 10.13 \times 10^4$ g/mol, run 3, 10 °C, [Al]/[Ni] = 600) among our three complexes. Complex **3b**, bearing a

naphthyl substituent in the *para*-aryl position of the ligand (only one methyl group in the *ortho*-aryl positions), exhibits a significantly lower catalytic activity and produces a lower molecular weight [run 12, the highest activity: 1.03×10^6 g PE/(mol Ni h bar); M_n : 7.86×10^4 g/mol]. These results indicate that the rate of chain

Table 3 Polymerization of ethylene with complexes **3a–c**/DEAC

| Run | Complex | [Al]/[Ni] | <i>T</i> (°C) | <i>t</i> (min) | Yield (g) | Activity ^a | TOF ^b (h bar) ⁻¹ | <i>M_n</i> (g/mol) | <i>M_w</i> / <i>M_n</i> ^c | Branches ^d /1,000 C | <i>D</i> ^e (nm) |
|-----|-----------|-----------|---------------|----------------|-----------|-----------------------|--|------------------------------|--|--------------------------------|----------------------------|
| 1 | 3a | 200 | 10 | 10 | 1.753 | 3.81 | 1.36 | 7.05 | 1.68 | – | – |
| 2 | 3a | 400 | 10 | 10 | 1.743 | 3.79 | 1.35 | 9.85 | 1.71 | – | – |
| 3 | 3a | 600 | 10 | 10 | 2.0377 | 4.43 | 1.58 | 10.13 | 1.74 | – | – |
| 4 | 3a | 800 | 10 | 10 | 1.986 | 4.32 | 1.54 | 6.45 | 1.78 | – | – |
| 5 | 3a | 1,000 | 10 | 10 | 1.9547 | 4.25 | 1.52 | 7.63 | 1.79 | – | – |
| 6 | 3a | 600 | 0 | 10 | 1.0089 | 2.19 | 0.78 | 9.68 | 1.72 | – | – |
| 7 | 3a | 600 | 20 | 10 | 1.2594 | 2.74 | 0.98 | 12.93 | 1.79 | 112 | 18.31 ± 2.1 |
| 8 | 3a | 600 | 40 | 10 | 0.8765 | 1.91 | 0.68 | 8.13 | 1.83 | 118 | 14.44 ± 1.9 |
| 9 | 3a | 600 | 60 | 10 | 0.4955 | 1.08 | 0.38 | 7.67 | 1.98 | 147 | 11.09 ± 1.5 |
| 10 | 3b | 200 | 10 | 10 | 0.378 | 0.79 | 0.28 | 4.34 | 1.68 | – | – |
| 11 | 3b | 400 | 10 | 10 | 0.4345 | 0.91 | 0.32 | 5.65 | 1.68 | – | – |
| 12 | 3b | 600 | 10 | 10 | 0.4954 | 1.03 | 0.37 | 7.86 | 1.70 | – | – |
| 13 | 3b | 800 | 10 | 10 | 0.4864 | 1.01 | 0.36 | 6.77 | 1.71 | – | – |
| 14 | 3b | 1,000 | 10 | 10 | 0.4129 | 0.86 | 0.31 | 6.21 | 1.77 | – | – |
| 15 | 3b | 600 | 0 | 10 | 0.2497 | 0.52 | 0.19 | 5.89 | 1.68 | – | – |
| 16 | 3b | 600 | 20 | 10 | 0.4732 | 0.96 | 0.35 | 9.05 | 1.75 | 113 | 12.29 ± 2.3 |
| 17 | 3b | 600 | 40 | 10 | 0.4059 | 0.85 | 0.30 | 5.93 | 1.81 | 127 | 8.98 ± 1.6 |
| 18 | 3b | 600 | 60 | 10 | 0.3762 | 0.78 | 0.28 | 4.10 | 1.95 | 151 | 6.27 ± 2.1 |
| 19 | 3c | 600 | 0 | 10 | 1.2976 | 1.30 | 0.46 | 10.03 | 1.71 | – | – |
| 20 | 3c | 600 | 20 | 10 | 0.9465 | 0.95 | 0.34 | 8.81 | 1.73 | 98 | 16.57 ± 3.1 |
| 21 | 3c | 600 | 40 | 10 | 0.6124 | 0.61 | 0.22 | 6.05 | 1.85 | 108 | 9.78 ± 2.9 |
| 22 | 3c | 600 | 60 | 10 | 0.4356 | 0.44 | 0.16 | 4.47 | 1.92 | 118 | 7.51 ± 2.2 |

Polymerization conditions: $n(\mathbf{3a}) = 2.23 \mu\text{mol}$, $n(\mathbf{3b}) = 2.24 \mu\text{mol}$, $n(\mathbf{3c}) = 5.00 \mu\text{mol}$, ethylene relative pressure = 0.2 bar, ethylene absolute pressure = 1.2 bar, *t* polymerization time, solvent = toluene (50 ml), *T* polymerization temperature

^a Activity in 10^6 g PE/(mol Ni h bar)

^b Turnover frequency in 10^5 mol Ethylene/(mol Ni h bar)

^c M_n in 10^4 g/mol, determined by GPC

^d Estimated by $^1\text{H NMR}$ [37]. Branches/1,000 C = $\frac{I_{\text{CH}_3}}{I_{\text{CH}_2} + I_{\text{CH}} + I_{\text{CH}_3}} \times 1,000$

^e Estimated by particle size analyzer

propagation is greatly promoted by the two *ortho*-methyl groups of the ligand's aryl rings. Complex **3c** bearing only two methyl groups in the *ortho*-aryl positions of the ligand [run 19, the highest activity: 1.30×10^6 g PE/(mol Ni h bar); Mn: 10.03×10^4 g/mol] exhibits an activity close to complex **3b**. This difference, observed between complex **3a** and **3c**, may be partially due to the presence of the naphthyl group in the *para*-aryl position of the ligand (naphthyl group may behave either as an electron donor or as an electron attractor). As a result, the following activity trend can be summarized for our substituted precatalysts under low ethylene pressure (0.2 bar), in the range 0–60 °C: **3a** > **3b** ~ **3c**.

Control of the polyethylene topology and size by α -diimine ligand structures and polymerization conditions

The type and amount of branches formed in the polymerization of ethylene promoted by typical α -diimine nickel precatalysts depend on reaction parameters such as the reaction temperature, ethylene pressure, and ligand structure [20]. Generally, low ethylene pressure and high polymerization temperature favor the Chain Walking mechanism and afford high branched polyethylenes [20]. However, the effect of ligand structure on polyethylene branching is much more complicated.

Recent studies by Guan and coworkers [38–40] demonstrated that in ethylene polymerization, the PE branching topology could be simply controlled by the pressure of ethylene, with linear PE being formed at high pressure and dendritic PE being obtained at low pressure. So, in this study, the low ethylene pressure (0.2 bar) was employed.

It is of particular interest that complexes **3a** and **3b** bearing the naphthyl substituent in the *para*-aryl position of the ligand produced the more dendritic polyethylenes than that of complex **3c** (Table 3; Fig. 3). The total branching degrees of the polymer samples prepared with **3a**/DEAC (runs 7–9, branching degree: 112, 118, and 147 branches/1,000 C at 20, 40, and 60 °C, respectively; diameter: 18.31, 14.44, and 11.09 nm at 20, 40, and 60 °C, respectively), and **3b**/DEAC (runs 16–18, branching degree: 113, 127, and 151 branches/1,000 C at 20, 40, and 60 °C, respectively; diameter: 12.29, 8.98, and 6.27 nm at 20, 40, and 60 °C, respectively) are much higher than that observed for **3c**/DEAC system (runs 20–22, branching degree: 98, 108, and 118 branches/1,000 C at 20, 40, and 60 °C, respectively; diameter: 16.57, 9.78, and 7.51 nm at 20, 40, and 60 °C, respectively). Also, the total branching degrees of the polymer samples prepared with **3a** and **3b**/DEAC are higher than those observed for similar precatalyst/DEAC systems such as {bis[*N,N'*-(4-*tert*-butyl-diphenyl)silyl]-2,6-diisopropylphenyl}imino]acenaphthene}dibromonickel (45 branches/1,000 C, at 20 °C) [20] or precatalyst/MAO systems such as

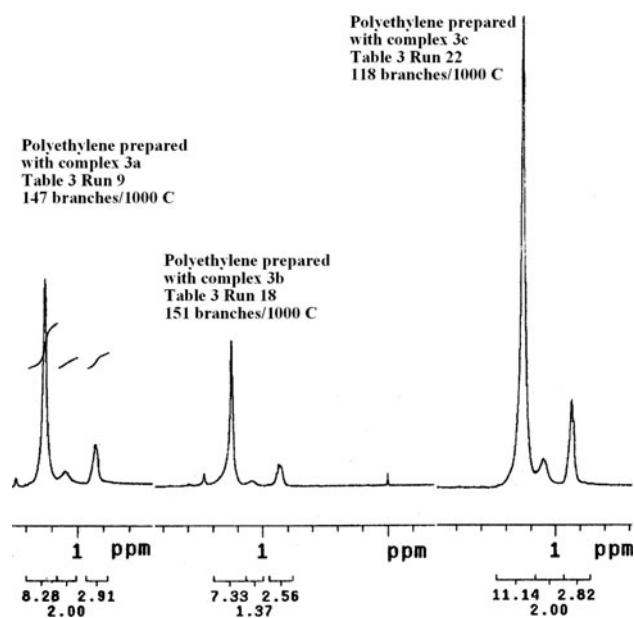


Fig. 3 ¹H NMR (CDCl₃/*o*-dichlorobenzene, v/v = 1:3) spectra of the nanosized dendritic polyethylene catalyzed by **3a**, **3b**, and **3c**/DEAC at 60 °C (Table 3, run 9, run 18, run 22). I_{CH_3} integrated intensity between 0.8 and 1.0 ppm, $I_{\text{CH}_2} + I_{\text{CH}}$: integrated intensity between 1.0 and 1.5 ppm

{bis[*N,N'*-(2,6-diisopropylphenyl)imino]-1,2-dimethylethane} dibromonickel (30, 67, 80, and 90 branches/1,000 C, at 25, 50, 65, and 80 °C, respectively) [20], and {bis[*N,N'*-(2,6-diisopropylphenyl)imino]acenaphthene}dibromonickel (65 branches/1,000 C, at 25 °C) [20], although the reaction conditions are not exactly the same as in the present work. A possible explanation is that the naphthyl group in the *para*-aryl position of the ligand (naphthyl group may behave either as an electron donor or as an electron attractor) may better stabilize the transition state for monomer chain walking than for insertion, which should afford a more dendritic polyethylene.

As shown in Fig. 4, the number of branches was also calculated according to the literature [41], and it was found that the polyethylene with 144 branches/1,000 carbons (99 methyl, 12 ethyl, 8 propyl, and 25 butyl or longer branches/1,000 C) was obtained at 60 °C (entry 8 in Table 3). This result was consistent with that calculated from ¹H NMR.

Conclusions

Two new α -diimine ligands **2a** and **2b**, and their Ni(II) complexes **3a** and **3b** have been prepared and characterized. Ligands **2a** and **2b** were modified in an attempt to change steric effects and the electronic density of the metal center and eventually to improve the activity in the polymerization of ethylene and control the microstructure and

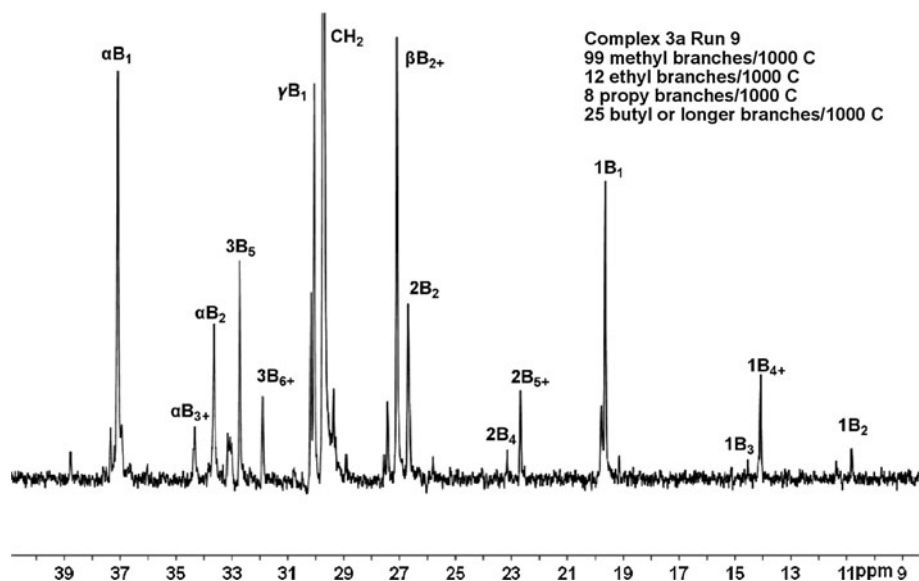


Fig. 4 ^{13}C NMR (CDCl_3 /*o*-dichlorobenzene, v/v = 1:3) spectrum of the nanosized dendritic polyethylene catalyzed by **3a**/DEAC at 60 °C (Table 3, run 9). Note on labels xBy B_y is a branch of length y carbons; x is the carbon being discussed, and the methyl at the end of the branch is numbered 1. Thus, the second carbon from the end of

a butyl branch is $2B_4$. xBy_+ refers to branches of length y and longer. The methylenes in the backbone are labeled with *Greek letters* which determine how far from a branch point methine each methylene is; α denotes the first methylene next to the methine. Thus, γB_{1+} refers to methylenes γ from a branch of length 1 or longer

size of the polyethylenes obtained. The results obtained show that complex **3a**, activated by DEAC, produces a highly active catalyst system for the polymerization of ethylene. Complexes **3a** and **3b** bearing the naphthyl substituent in the *para*-aryl position of the ligand produced more nanosized dendritic polyethylene. A ligand bearing a naphthyl group in the *para*-aryl position (naphthyl group may behave either as an electron donor or as an electron attractor) may better stabilize the transition state for monomer chain walking than for insertion, which should afford a more dendritic polyethylene.

Supplementary material

CCDC 905358 and 905359 contain the supplementary crystallographic data for ligand **2a** and complex **3a**. These data can be obtained free of charge via <http://www.ccdc.cam.ac.uk> or from the Cambridge Crystallographic Data Centre, 12 Union Road, Cambridge CB2 1EZ, UK; fax: (+44) 1223-336-033; or e-mail: deposit@ccdc.cam.ac.uk.

Acknowledgments We thank the National Natural Science Foundation of China (20964003), Chinese Ministry of Education Returned Overseas Students Scientific Research Foundation (2009-1341), and Chinese Ministry of Human Resources and Social Security Overseas Students Science and Technology Activities Merit-based Foundation (2009-416) for funding.

References

- Sun G, Hentschel J, Guan Z (2012) ACS Macro Lett 1:585–588
- Zhang Z, Ye Z (2012) Chem Commun 48:7940–7942
- Killian CM, Tempel DJ, Johnson LK, Brookhart M (1996) J Am Chem Soc 118:11664–11665
- Popeney CS, Lukowiak MC, Böttcher C, Schade B, Welker P, Mangoldt D, Gunkel G, Guan Z, Haag R (2012) ACS Macro Lett 1:564–567
- Gao H, Hu H, Zhu F, Wu Q (2012) Chem Commun 48:3312–3314
- Shi X, Zhao Y, Gao H, Zhang L, Zhu F, Wu Q (2012) Macromol Rapid Commun 33:374–379
- Johnson LK, Killian CM, Brookhart M (1995) J Am Chem Soc 117:6414–6415
- Yuan JC, Mei TJ, Gomes PT, Marques MM, Wang XH, Liu YF, Miao CP, Xie XL (2011) J Organomet Chem 696:3251–3256
- Yuan JC, Silva LC, Gomes PT, Campos JM, Riberio MR, Valerga PS, Chien JCW, Marques MM (2005) Polymer 46:2122–2132
- Peleška J, Hošťálek Z, Hasalíková D, Merna J (2011) Polymer 52:275–281
- Wegner MM, Ott AK, Rieger B (2010) Macromolecules 43:3624–3633
- Choi Y, Soares JBP (2010) Polymer 51:2271–2276
- Camachoa DH, Guan Z (2010) Chem Commun 46:7879–7893
- Guan Z, Popeney CS (2009) Top Organomet Chem 26:179–220
- Takeuchi D, Fukuda Y, Park S, Osakada K (2009) Macromolecules 42:5909–5912
- Li L, Jeon M, Kim SY (2009) J Mol Catal A Chem 303:110–116
- Popeney C, Guan Z (2005) Organometallics 24:1145–1155
- Liu FS, Hu HB, Xu Y, Guo LH, Zai SB, Song KM, Gao HY, Zhang L, Zhu FM, Wu Q (2009) Macromolecules 42:7789–7796

19. Cherian AE, Rose JW, Lobkovsky EB, Coates GW (2005) *J Am Chem Soc* 127:13770–13771
20. Ittel SD, Johnson LK, Brookhart M (2000) *Chem Rev* 100:1169–1203
21. Johnson LK, Mecking S, Brookhart M (1996) *J Am Chem Soc* 118:267–268
22. Mecking S, Johnson LK, Wang L, Brookhart M (1998) *J Am Chem Soc* 120:888–899
23. Gottfried AC, Brookhart M (2003) *Macromolecules* 36:3085–3100
24. Schrekker HS, Kotov V, Preishuber-Pflugl P, White P, Brookhart M (2006) *Macromolecules* 39:6341–6354
25. Yang WJ, Cheng YY, Xu TW, Wang XY, Wen LP (2009) *Eur J Med Chem* 44:862–868
26. Svenson S, Tomalia DA (2005) *Adv Drug Deliv Rev* 57:2106–2129
27. Matsumura Y, Maeda H (1986) *Cancer Res* 46:6387–6392
28. Maeda H, Sawa T, Konno T (2001) *J Control Release* 74:47–61
29. Maeda H, Bharate GY, Daruwalla J (2009) *Eur J Pharm Biopharm* 71:409–419
30. Danhier F, Feron O, Préat V (2010) *J Control Release* 148:135–146
31. Gillies ER, Fréchet JMJ (2005) *Drug Discov Today* 10:35–43
32. Chen G, Huynh D, Felgner PL, Guan Z (2006) *J Am Chem Soc* 128:4298–4302
33. Ward LGL, Pipal JR (1972) *Inorg Synth* 13:162–163
34. Van KG, Vrieze K (1982) *Adv Organomet Chem* 21:151–239
35. Song CL, Tang LM, Li YG, Li XF, Chen J, Li YS (2006) *J Polym Sci Pol Chem* 44:1964–1974
36. Maldanis RJ, Wood JS, Chandrasekaran A, Rausch MD, Chien JCW (2002) *J Organomet Chem* 645:158–167
37. Meinhard D, Wegner M, Kipiani G, Hearley A, Reuter P, Fischer S, Marti O, Rieger B (2007) *J Am Chem Soc* 129:9182–9191
38. Guan Z, Cotts PM, McCord EF, McLain SJ (1999) *Science* 283:2059–2062
39. Guan Z (2002) *Chem Eur J* 8:3086–3092
40. Cotts PM, Guan Z, McCord EF, McLain SJ (2000) *Macromolecules* 33:6945–6952
41. Galland GB, Souza RF, Mauler RS, Nunes FF (1999) *Macromolecules* 32:1620–1625